Applied Surface Science 357 (2015) 248–254

Contents lists available at ScienceDirect

Applied Surface Science

journal homepage: www.elsevier.com/locate/apsusc

Nanosecond laser textured superhydrophobic metallic surfaces and their chemical sensing applications

Duong V. Ta[a,*], Andrew Dunn[a], Thomas J. Wasley[b], Robert W. Kay[b], Jonathan Stringer[c], Patrick J. Smith[c], Colm Connaughton[d], Jonathan D. Shephard[a]

[a] Institute of Photonics and Quantum Sciences, Heriot-Watt University, Edinburgh EH14 4AS, UK
[b] Additive Manufacturing Research Group, Loughborough University, Leicestershire LE11 3TU, UK
[c] Laboratory of Applied Inkjet Printing, Department of Mechanical Engineering, University of Sheffield, Sheffield S1 4BJ, UK
[d] Warwick Mathematics Institute and Centre for Complexity Science, University of Warwick, Zeeman Building, Coventry CV4 7AL, UK

ARTICLE INFO

Article history:
Received 4 June 2015
Received in revised form 27 August 2015
Accepted 1 September 2015
Available online 3 September 2015

Keywords:
Superhydrophobic surface
Nanosecond laser
Metal
Chemical sensor

ABSTRACT

This work demonstrates superhydrophobic behavior on nanosecond laser patterned copper and brass surfaces. Compared with ultrafast laser systems previously used for such texturing, infrared nanosecond fiber lasers offer a lower cost and more robust system combined with potentially much higher processing rates. The wettability of the textured surfaces develops from hydrophilicity to superhydrophobicity over time when exposed to ambient conditions. The change in the wetting property is attributed to the partial deoxidation of oxides on the surface induced during laser texturing. Textures exhibiting steady state contact angles of up to ~152° with contact angle hysteresis of around 3–4° have been achieved. Interestingly, the superhydrobobic surfaces have the self-cleaning ability and have potential for chemical sensing applications. The principle of these novel chemical sensors is based on the change in contact angle with the concentration of methanol in a solution. To demonstrate the principle of operation of such a sensor, it is found that the contact angle of methanol solution on the superhydrophobic surfaces exponentially decays with increasing concentration. A significant reduction, of 128°, in contact angle on superhydrophobic brass is observed, which is one order of magnitude greater than that for the untreated surface (12°), when percent composition of methanol reaches to 28%.

1. Introduction

Controlling surface wettability has attracted increased research attention due to the wide range of applications ranging from domestic innovations such as self-cleaning glass to high-technology fields like microfluidic control, corrosion resistance, water–oil separation and drag reduction [1–4]. New applications are continuously being discovered, for instance, the use of low wetting surfaces for the realization of microdroplet lasers [5,6]. Recently, the developments in designing and preparing novel surfaces with special wettability have opened opportunities to employ these surfaces for liquid transportation and smart sensing devices [7,8].

Today, superhydrophobic surfaces on glasses, semiconductors, polymers and metals can be generated by various methods, including lithography, plasma treatment, chemical deposition, colloidal assembling, templating, and ultrafast laser surface texturing [9]. Among these options, laser patterning is a promising method due to the potentially high fabrication speeds, low waste and maskless single-step processing [10–13]. This technology is also highly suitable for producing superhydrophobic surfaces with selective area patterning [14,15].

Superhydrophobic metallic surfaces based on laser texturing have been investigated previously [16,17]. However, to date, most of the reported works rely on high-cost, complex ultrafast (femto-/pico-second) lasers [16–23]. For these lasers, the pulse energy is relatively low so high pulse overlapping is required for creating the surface modification and therefore processing rates are slow. For real industrial applications, the ability to create superhydrophobic metallic surfaces using compact, robust and cost–effective alternatives with fast processing times, such as nanosecond fiber lasers, would be highly desirable.

Copper and brass are widely used for electronic components and industrial devices due to their high electrical and thermal conductivity. However, they are easily affected by environmental conditions, such as high humidity leading to corrosion. Recently, it

* Corresponding author.
E-mail address: d.ta@hw.ac.uk (D.V. Ta).

http://dx.doi.org/10.1016/j.apsusc.2015.09.027

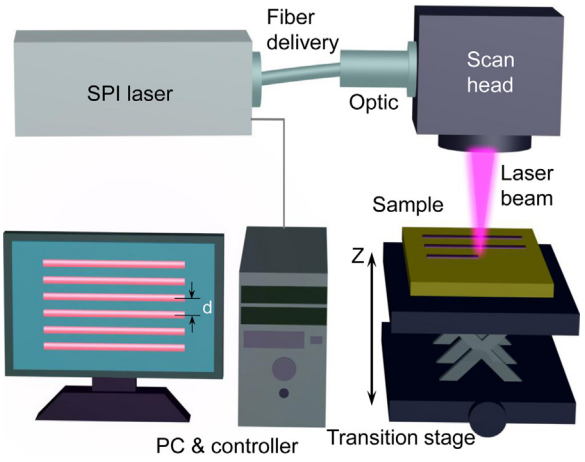

Fig. 1. Schematic of optical setup for fabrication of microgroove structures on copper and brass surfaces.

has been shown these problems can be prevented on these materials by creating a superhydrophobic surface [24].

In this paper, the superhydrophobic behavior of copper and brass surfaces achieved by infrared nanosecond laser surface texturing is presented. The superhydrophobic surfaces demonstrate the self-cleaning properties and have potential for liquid chemical sensing applications.

2. Experimental

2.1. Materials

The experiments detailed in this paper were performed on commercially available copper (purity 99.9%) and brass sheets (RS Components, CZ121M, 58% Cu, 39% Zn, and 3% Pb) with thicknesses of 0.45 and 0.6 mm, respectively. Prior to laser radiation, the samples were cleaned with isopropanol.

2.2. Surface laser irradiation

Hierarchical structures on the sample surface were fabricated using a SPI fiber laser (20 W EP-S) system including a galvanometer scanning system to move the beam over the surface as shown in Fig. 1 [25]. Arrays of microgroove structures were directly written on the sample surface. The distance between adjacent microgrooves (pitch size, d) was kept constant. The sample was irradiated, normal to the surface, by the fiber laser with nominal beam spot of about 21 μm, wavelength of 1064 nm and pulse width of ~220 ns. A scanning speed of 75 mm/s and repetition rate of 25 kHz were used. This processing rate is about two orders of magnitude higher compared with that using femtosecond lasers [16,18]. Three different fluences were applied separately to the work piece for copper (75, 84, 93 J/cm^2) and brass (55, 65, 75 J/cm^2).

2.3. Surface analysis

The samples were left in air, under ambient conditions before studying their surface wettability by measuring the contact angle. A ~5 μL droplet of deionized water was dispensed onto the sample surface using a syringe while an image was captured by a camera (Unibrain 1394) combined with a 12× magnification system. The contact angle (θ) was then determined by analyzing the droplet images using the software FTA32 (version 2.0). The contact angle hysteresis ($\Delta\theta$) was estimated by comparing the advancing and receding contact angle. The rolling-off angle was estimated as the tilted superhydrophobic surface on which deposited droplets start to rolling downwards. In order to study the surface morphology of the laser textured samples, scanning electron microscopy (SEM) and optical microscopy (Leica DM6000M) were used. The chemical composition of the surface was investigated by energy-dispersive X-ray (EDX) measurements.

2.4. Chemical solution for sensing demonstration

Methanol (99.5% purity) was dissolved in deionized water to form methanol solutions with various concentrations. ~5 μL droplets of these solutions were dispensed on laser textured brass surfaces that had previously been exposed to ambient conditions for 38 days. The contact angle was determined as described in Section 2.3.

3. Results and discussion

3.1. The effect of laser irradiation on surface structure

Prior to fabricating the microgroove structures, the effect of individual pulses on the surface was studied. Fig. S1 shows the near-circular craters induced on the copper surface by single pulses of laser radiation. The craters are formed due to the rapid heating of the copper, resulting in melting and evaporation (ablation), at the location of the laser radiation. Most of the material from the center of the crater was redeposited in the area surrounding the crater. The total amount of removed material depends on laser fluence. Fig. S1b–d shows the increase of crater diameter from about 24 μm under 75 J/cm^2 to 30 μm under 93 J/cm^2. The crater depth (determined by optical microscopy) also increased from around 4 to 6 μm, respectively. Similarly, Fig. S2 present craters on brass surface irradiated with three fluences. The crater diameter on brass increased from approximately 27 to 30 μm under fluence of 55 and 75 J/cm^2, respectively. The crater depth was around 3–5 μm.

Fig. S3 shows how microgroove structures can be created by increasing overlap of laser spot. The same scanning speed at 75 mm/s was applied while the repetition rate of the laser was varied from well separated pulses (Fig. S3a) to partly (Fig. S3b) and highly (Fig. S3c) overlapping. With a repetition rate of 25 kHz, the microgroove structure was formed with a significant amount of recast material around the perimeter of the feature. Fig. 2a shows a SEM image of the completed microgrooves on brass, irradiated with 65 J/cm^2, demonstrating the effect of the laser radiation on creating regular microstructures with micro-roughness on the sample's surface. Depth of the microgrooves on copper and brass surfaces, measured using optical microscopy, varied from around 10 to 25 μm, depending on laser fluence. Fig. 2b shows a three-dimensional image of the structure on brass surface irradiated with 65 J/cm^2 indicating that the depth of microgrooves was about 20 μm. It is noted that, due to high pulse overlap, the depth of the channels is larger than that of the craters created by a single pulse.

3.2. Time effects on surface wettability

The laser treated surfaces becomes hydrophilic immediately after fabrication (see Supporting Video 1 for more information). However, the surface wettability decreases over time, as indicated by the increase in contact angle. The first measurement after processing was made after the samples were left under ambient conditions for 3 days. Fig. 3 plots the evolution of contact angle with time for copper and brass samples with d = 75 μm, irradiated by three different fluences. Each data point presented is average value of three individual measurements. It can be seen that the contact angle exhibits a sharp increase during the first ten days, which then slows to a gradual growth before finally reaching a steady

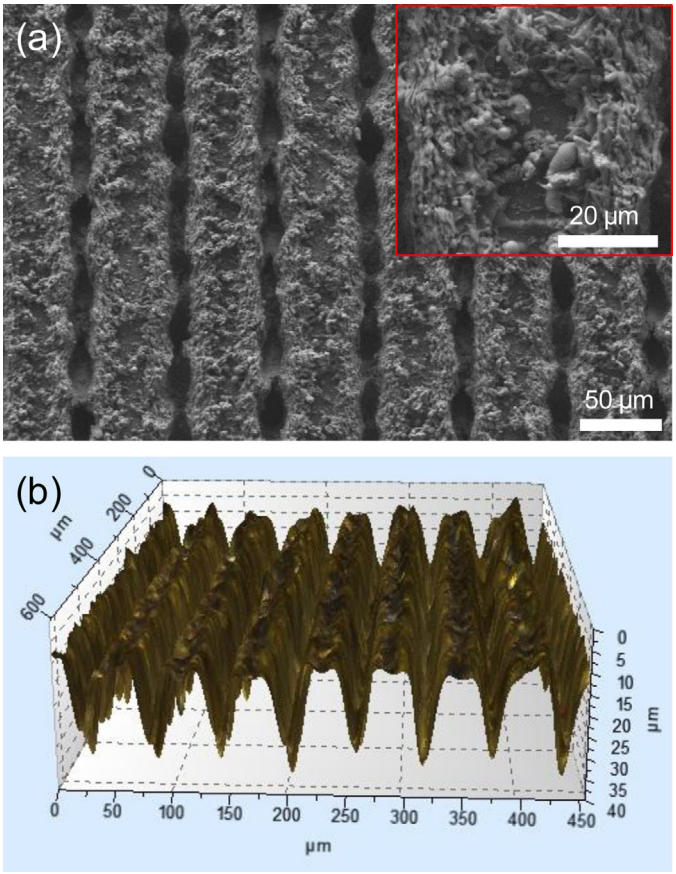

Fig. 2. Scanning electron microscope (SEM) and microscopy images of the laser textured brass surface irradiated with 65 J/cm^2, d = 75 μm. (a) The SEM image show laser induced microgrooves. Higher magnification is presented in the inset indicating micro-/nano roughness. (b) Microscopy image obtained by focus stacking of optical images showing surface structures and depth of the microgrooves.

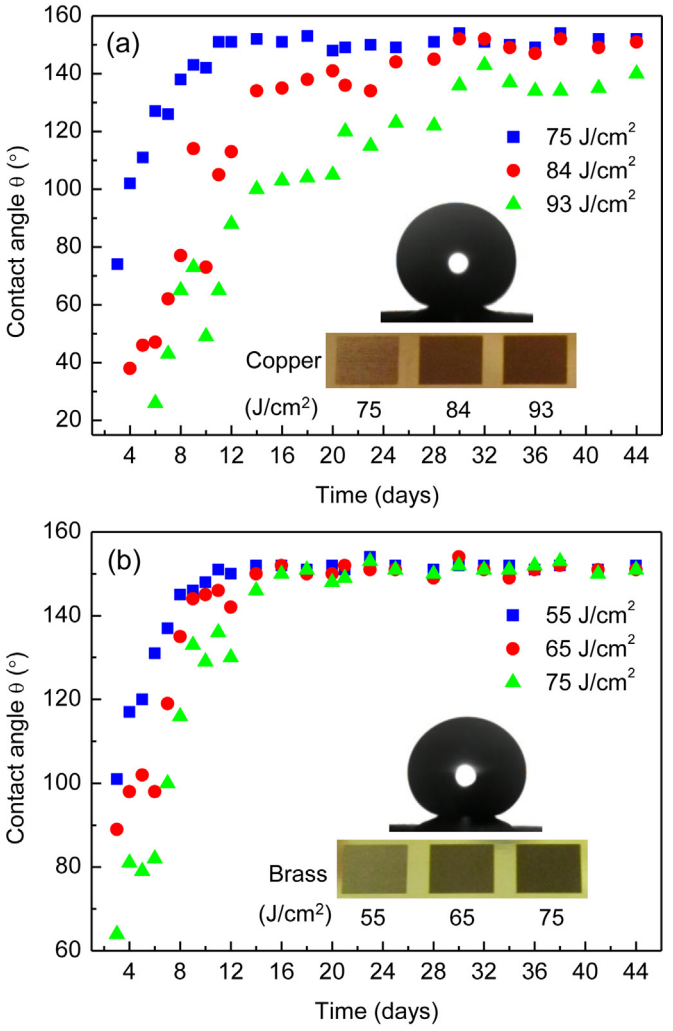

Fig. 3. Contact angle development over time for various fluences. (a) Copper and (b) brass surfaces. Optical images of the samples with corresponding laser fluence are shown in the insets along with images of droplets on a surface with high contact angle.

state. The steady state was reached after about 11 days for copper and brass samples irradiated with 75 and 55 J/cm^2, respectively. However, it took much longer, approximately 30 days, for copper irradiated with 93 J/cm^2.

Similar to ref. [16], the development of the contact angle over time is found to be well-fitted (as shown in Fig. 4a) with an exponential growth function expressed as: $\theta = \theta_{eq}(1 - \exp(-t/\beta))$, where θ_{eq} and β are equilibrium (steady state) contact angle and time constant, respectively. It is noted that the value of θ_{eq} was self-estimated for reducing standard error of β (which indicates the time when the contact angle reaches 63% of its maximum).

Fig. 4b and c plots θ_{eq} and β for copper and brass samples, respectively. It can be seen that the equilibrium contact is slightly above 150° for all samples except the copper irradiated by 93 J/cm^2. Samples irradiated with the lowest fluences (55 J/cm^2 for brass and 75 J/cm^2 for copper) develop from hydrophilic to superhydrophobic much faster than samples treated by higher fluences, which has been similarly observed in other metals [16]. For copper, the time constant was 3.7 days under 75 J/cm^2. This value significantly increased to 13.5 days for samples irradiated with 93 J/cm^2, an increase of nearly 265%. The evolution process was faster for brass samples, which took 2.9 and 5.6 days to reach 63% of steady state contact angle for fluences of 55 and 75 J/cm^2, respectively.

Thermodynamic modeling has proven that the level of superhydrophobicity depends on groove depth and pitch size [26]. In this work, due to increased groove depth and strong modification of surface chemistry, the surface wettability was found to increase with laser fluence. To investigate the effect of pitch size on the surface wettability, laser fluence was kept constant while the pitch size was changed. Fig. 5 compares the evolution from hydrophilicity to hydrophobicity of brass sample irradiated with 75 J/cm^2 for various d ranging from 25 to 100 μm. Although the equilibrium contact angles for all samples were similar (approximately 152°), their time constants were different. The samples with larger d (100 and 75 μm) appear to become hydrophobic faster than those with smaller d (50 and 25 μm).

It has been demonstrated that, although the laser textured copper and brass surfaces become hydrophilic directly after fabrication, the wettability changes to hydrophobic over time. This effect is highly reproducible. Fig. S4 compares the development from hydrophilicity to hydrophobicity for two different set of brass samples with d = 75 μm and irradiated with 75 J/cm^2 (the data has been presented in Fig. 3b and Fig. 5). The result indicates very similar evolution trends.

3.3. Superhydrophobic behavior

A high contact angle (>150°) is only one important characteristic of a superhydrophobic surface. Another vital factor is small contact angle hysteresis or rolling-off angle (not exceeding 10°) [27]. This value can be measured by comparing advancing and receding

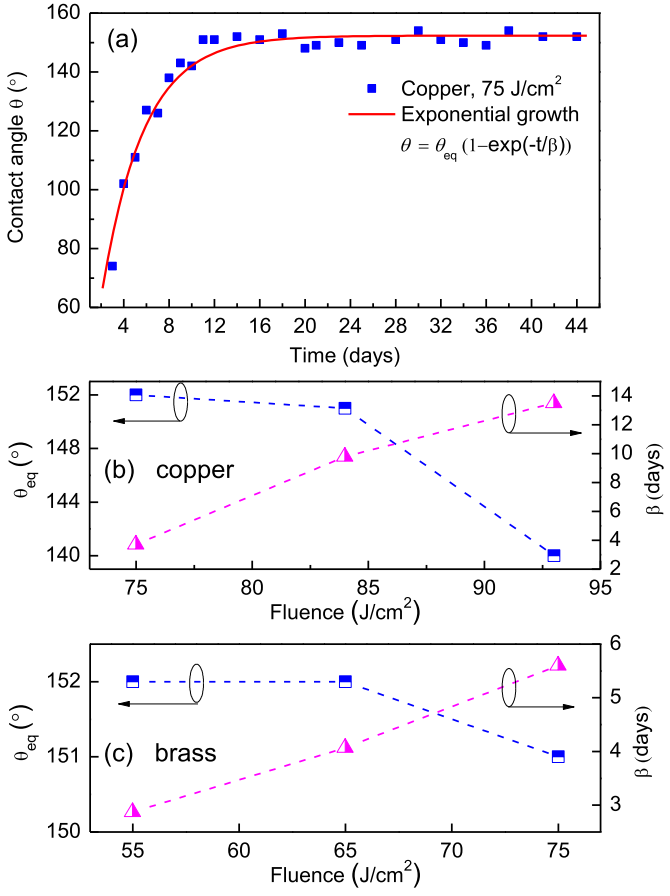

Fig. 4. Characteristics of the contact angle development for textured copper and brass surfaces. (a) Exponential growth behavior of contact angle over time of textured copper samples irradiated with 75 J/cm^2. (b, c) Contact angle equilibrium (θ_{eq}) and their coefficient time constant (β) as function of fluences.

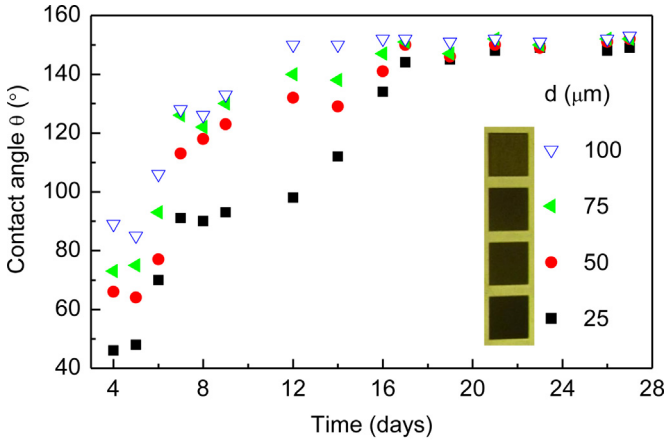

Fig. 5. Contact angle evolution of textured brass surfaces versus pitch size. The inset show optical images of samples with corresponding pitch size.

angles of a droplet on a tilted surface [9]. Alternatively, it can be determined by subtracting the two contact angles of growing and shrinking droplets [16]. Fig. 6 shows dynamic of contact angle on a brass surface irradiated by 55 J/cm^2 after it reaches steady stage (see Supporting Video 2 for demonstration of the process). First, the droplet was suspended from a syringe (Fig. 6a) and then made to contact the surface by lifting up the sample with a translation stage (Fig. 6b). The droplet did not wet the surface and exhibits sliding on the surface when the substrate reached a certain height (Fig. 6c). The droplet then deformed when the surface is lowered (Fig. 6d and e) and finally departed from the surface (Fig. 6f). This behavior is found to be the same for all textured copper and brass samples. It indicates that there was negligible adhesion between the droplet and the surface and, therefore, suggests $\Delta\theta$ is small. Actually, the contact angle before the droplet begins sliding on (Fig. 6b) and departing from (Fig. 6e) the surface can be considered as maximum and minimum static contact angles, and these values should be close to advancing and receding contact angles, respectively. With this consideration, it is estimated $\Delta\theta$ for all samples was found to be in a range of 3–4°, which meets the requirement of a superhydrophobic surface.

The obtained low value of $\Delta\theta$ is supported by rolling-off angle measurements. Fig. 7 shows a time sequence of a droplet rolling on a 2.9° tilted hydrophobic brass surface irradiated with 55 J/cm^2 (see Supporting Video 3 for a demonstration of the process). The droplet was suspended then dropped from a syringe and started rolling down the incline on contact with the surface with rolling speed of about 8 cm/s. It was also found that rolling-off angle for many of the samples could be as small as 2°. The potential to create such laser textured superhydrophobic surfaces on copper or brass could

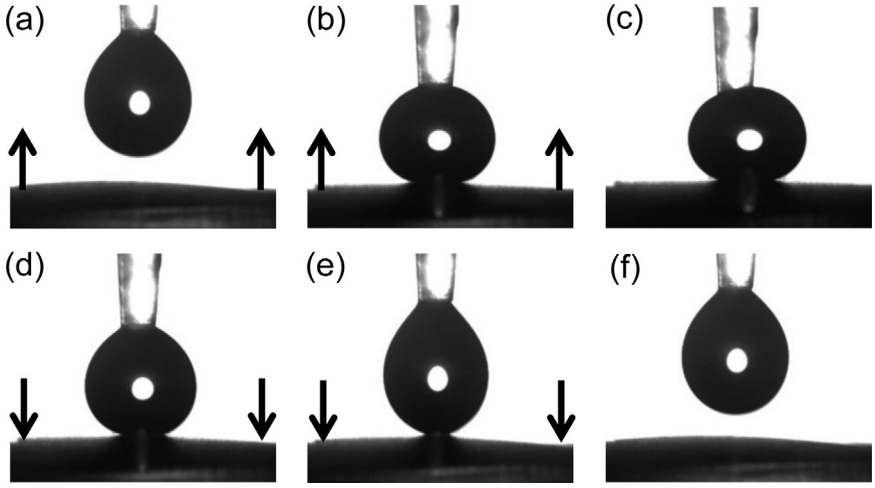

Fig. 6. Low adhesion between droplet and hydrophobic surface indicates small contact angle hysteresis. (a) ~5 μL water drop suspended on a syringe. (b) Strongly contacted with the lifting surface and (c) starting to slide on the surface due to the increase of upward force. (d, e) The distortion of droplet increases by lowering the surface and (f) droplet finally departed from the surface without wetting.

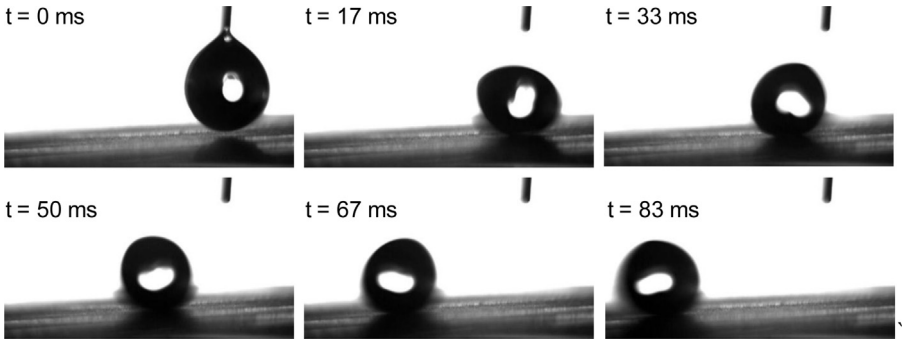

Fig. 7. Time sequence of a droplet rolling on a 2.9° tilted hydrophobic brass surface irradiated with 55 J/cm^2.

enable the fabrication of devices which are highly water resistant, potentially improving corrosion resistance [24].

3.4. Explanation of change in wettability

Wettability of rough surfaces has been under investigation for decades [28,29] and the change in wettability of metallic surfaces due to laser texturing and after exposing to the air has been previously reported [16]. Several mechanisms have been proposed such as the decomposition of carbon dioxide into carbon with active magnetite, adsorption of organic matter from the atmosphere and creation of hydrophobic groups [16,30,31]. In our work, directly after fabrication, the surfaces exhibit hydrophilic behavior with very small contact angles. This effect is attributed to the modification of both surface morphology and surface chemistry during the laser processing. Roughness was introduced via ablation (vaporization) which increases the wettability accordingly to the Wenzel equation [28].

$$\cos\theta_w = r\cos\theta_f \quad (1)$$

where, $r > 1$ is the roughness factor. θ_w and θ_f are contact angles on rough and flat surfaces, respectively. Eq. (1) also predicts the change in surface chemistry, which induces $\Delta\theta_f$, would lead to a change in $\Delta\theta_w$ (Wenzel contact angle on a rough surface) as follows [32]:

$$\Delta\theta_w = r(\sin\theta_f / \sin\theta_w)\Delta\theta_f \quad (2)$$

Fig. 8 shows that the oxygen composition increased sharply from about 3.6% for the unprocessed substrate to 9.0 and 20.2% when irradiated by fluences of 55 and 75 J/cm^2, respectively. During the laser texturing, it is proposed that layers of CuO and ZnO were formed by the reaction between copper and zinc with oxygen. The formation of CuO (a hydrophilic material [33]), in conjunction with the roughness, should increase the wettability of laser textured surfaces and therefore explains the high wetting behavior observed on the surfaces shortly after processing with laser radiation.

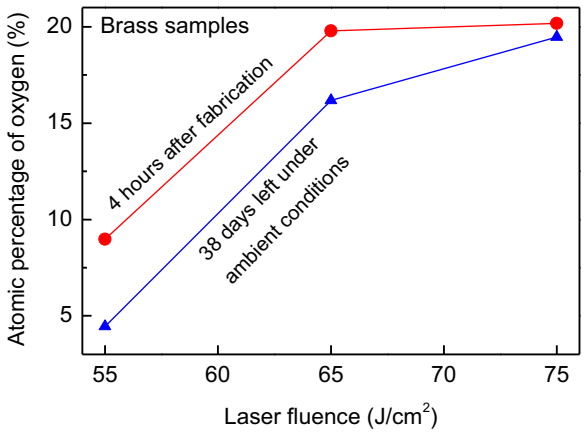

Fig. 8. Oxygen composition on three laser textured brass surfaces (irradiated with 55, 65 and 75 J/cm^2) measured (i) directly after fabrication and (ii) after being left under ambient conditions for 38 days.

However, when exposed to ambient conditions the wettability of the laser textured surfaces changed with time. This phenomenon is ascribed to modification of the surface chemistry as there is no change in surface morphology over time. Even though the adsorption of organic matter from the atmosphere [31] is a considerable factor, measurements suggest that the deoxidation proposed by Chang et al. [33] should effectively contribute to the development from hydrophilic to superhydrophobic. Fig. 8 indicates decrease of the oxygen component (from 9.0 to 4.5%, 19.8 to 16.2%, and 20.2 to 19.5%, for fluences of 55, 65 and 75 J/cm^2, respectively) after leaving the samples under ambient conditions for 38 days. This observation is understandable by the partial deoxidation of CuO into Cu_2O ($2CuO \leftrightarrow Cu_2O + 1/2O_2$) [33]. It is suggested that the deoxidation of the CuO is a heterogeneous nucleation and growth mechanism that initiates at defects, therefore the surface will consist of different regions of different wettability (CuO and Cu_2O) that are of a scale much smaller than the droplet. The mole ratio of Cu_2O to CuO increases with time, and as Cu_2O is a hydrophobic material [33], the deoxidation process causes the change in wetting behavior. It is noted that we did not observe a clear relationship between the surface wettability and carbon content, as discussed previously [16]. When the contact angle reaches a steady state, the surface wetting becomes incomplete, suggesting a transition from Wenzel to Cassie–Baxter regime. The contact angle of droplets now can be described by the general Cassie–Baxter equation [29].

$$\cos\theta_{C-B} = f_1(x,y)\cos\theta_1 + f_2(x,y)\cos\theta_2 \quad (3)$$

where f_1 and f_2 are local densities, function of surface (x, y) coordinates. $f_1 + f_2 = 1$. θ_1 and θ_2 are contact angles corresponding to Cu_2O (suppose that the Cu_2O is dominant to CuO) and air. It is noted that the deoxidation mechanism also provides an explanation for the observation that samples irradiated with a lower fluence become superhydrophobic more quickly as it is expected that for low incident energy the CuO layers are thinner which make them transition to Cu_2O more readily.

3.5. Self-cleaning effect

Self-cleaning is an important application of superhydrophobic surfaces. This effect is exploited in nature in many plants because it helps to wash away contaminants and acts as a defense against pathogens [34]. For artificial superhydrophobic surfaces self-cleaning behavior is also has significant benefit for practical applications [1]. Consequently, the nanosecond laser surface texturing process developed for copper and brass in this work is a viable route to achieving this property. In Supporting Video 4, the

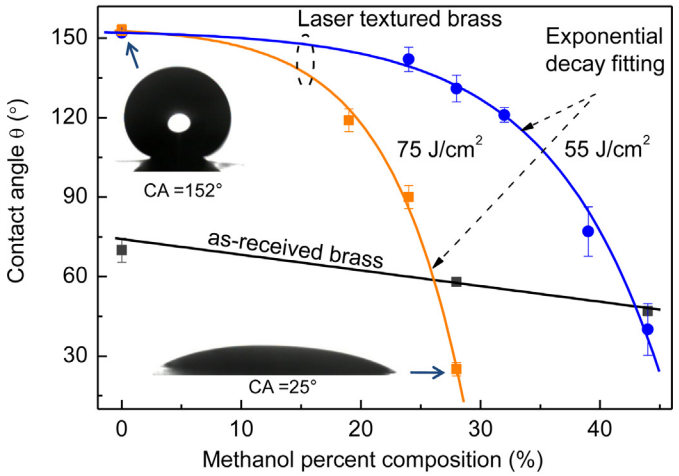

Fig. 9. Contact angle of methanol/water solution on unprocessed as-received brass substrate and superhydrophobic brass surfaces (left under ambient conditions for 38 days after fabrication) irradiated with 55 and 75 J/cm^2.

self-cleaning effect on a 6° tilted superhydrophobic brass surface is demonstrated. $CaCO_3$ powder served as a contaminant on the surface [24]. Water droplets were dropped on to the top part of the surface where they rolled quickly down to the bottom, taking away the fine particles. The dusty surface became clean after depositing several of droplets. In comparison, the unprocessed surface (central region of the sample) did not exhibit the self-cleaning ability and droplets remained on the surface due to strong adhesion.

3.6. Chemical sensing applications

Superhydrophobic surfaces have also been considered for sensing applications such as thermal and pH sensors [35,36]. In this work, the potential of using the nanosecond laser textured superhydrophobic surfaces for a novel chemical sensing application is demonstrated.

It is well known that the wettability of a surface is not only dependent on the surface morphology and chemistry but also on the liquid [37]. Due to the smaller surface tension for less polar liquids compared with water, the contact angle of water droplets can be much higher than droplets of less polar liquids (such as octane and methanol) on the same surface [37]. It therefore follows that, for solutions which are mixtures of water and a less polar liquid, the contact angle should decrease with increase of concentration of the less polar liquid. As a result, a solution concentration can be determined by simply monitoring the contact angle and hence provides a mechanism to develop chemical sensors.

Fig. 9 compares the contact angle of a methanol/water solution on an unprocessed as-received brass substrate and superhydrophobic brass surfaces irradiated with 55 and 75 J/cm^2 and left in ambient conditions for 38 days. Again, each data point presented is an average value of three individual measurements. It is clear that the contact angle decreased with increasing methanol concentration. The relationship was well fitted with a linear function for the unprocessed substrate which exponentially decays for the laser textured surfaces. When the concentration rose from 0 to 15%, a slight reduction in the contact angle for all samples is expected. However, at higher concentrations, a significant decrease in contact angle was observed for the nanosecond laser textured samples. When the concentration is increased from 0% to 44%, the contact angle drops sharply from 150° to 40° for a sample irradiated with 55 J/cm^2, a major decrease of 110° compared with 24° (from 70° to 46°) for the unprocessed sample. The sample irradiated with 75 J/cm^2 demonstrated the highest sensitivity. There was a significant decrease of 128° in contact angle (from 153° to 25°), which is one order of magnitude higher compared with only 12° for the unprocessed surface, when concentration of methanol reaches 28%. The drop in contact angle of the methanol solutions due to surface tension change is enhanced by the roughness factor. It is noted that the sensing process does not appear to be completely reversible. Substrates used for the sensing measurement lose their superhydrophobic properties after the experiment. The methanol solution seems to chemically modify the hydrophobic surface, thus resulting in lower contact angles and it appears to be a one-way reaction. The change is not entirely permanent; the surface wettability decreases when exposed to the air afterwards, but the development of this process is extremely slow compared with that of new laser structured surfaces.

4. Conclusions

It has been shown that textured superhydrophobic surfaces on copper and brass can be achieved by using a compact and cost effective nanosecond fiber laser. Directly after fabrication, the samples exhibit hydrophilic behavior but gradually become superhydrophobic over time with the maximum contact angle being achieved after ~11 days. The hydrophilic property is ascribed to the laser induced roughness. However, this role of surface morphology changes over time, which results in the surfaces becoming superhydrophobic. The change in wettability is due to surface chemistry, in which partial deoxidation of CuO into Cu_2O on the surface is likely a key factor. The steady state contact angle is about 152° with low contact angle hysteresis of 3–4°. The superhydrophobic surfaces have been demonstrated to exhibit self-cleaning behavior and show potential for liquid chemical sensing applications. The sensor's sensitivity is defined as the decrease of contact angle with increase of chemical concentration. The sensitivity for superhydrophobic surfaces is one order of magnitude higher compared with that for unprocessed surface. Overall, this work demonstrates a cost effective, direct write, environmentally friendly (low waste) and fast processing method to modify wettability of common metals for multifunctional applications.

Data availability

All relevant data present in this publication can be accessed at http://dx.doi.org/10.17861/0363e95e-e67f-4d22-aca9-c4aa4a8dd7c2.

Acknowledgements

We thank Dr. Jim Buckman for helping with SEM and EDX measurements. This work is funded by the UK Engineering and Physical Sciences Research Council under grants EP/L017431/1, EP/L017350/1, EP/L016907/1 and EP/L017415/1.

Appendix A. Supplementary data

Supplementary material related to this article can be found, in the online version, at http://dx.doi.org/10.1016/j.apsusc.2015.09.027

References

[1] R. Blossey, Self-cleaning surfaces-virtual realities, Nat. Mater. 2 (2003) 301–306.
[2] K.-C. Park, H.J. Choi, C.-H. Chang, R.E. Cohen, G.H. McKinley, G. Barbastathis, Nanotextured silica surfaces with robust superhydrophobicity and omnidirectional broadband supertransmissivity, ACS Nano 6 (2012) 3789–3799.

[3] X. Zhang, F. Shi, J. Niu, Y. Jiang, Z. Wang, Superhydrophobic surfaces: from structural control to functional application, J. Mater. Chem. 18 (2008) 621–633.
[4] R. Truesdell, A. Mammoli, P. Vorobieff, F. van Swol, C.J. Brinker, Drag reduction on a patterned superhydrophobic surface, Phys. Rev. Lett. 97 (2006) 044504.
[5] A. Kiraz, M.A. Duendar, A.L. Demirel, S. Doganay, A. Kurt, A. Sennaroglu, M.Y. Yuece, Single glycerol/water microdroplets standing on a superhydrophobic surface: optical microcavities promising original applications, J. Nanophotonics 1 (2007) 011655.
[6] V.D. Ta, R. Chen, H.D. Sun, Self-assembled flexible microlasers, Adv. Mater. 24 (2012) OP60–OP64.
[7] B.W. Xin, J.C. Hao, Reversibly switchable wettability, Chem. Soc. Rev. 39 (2010) 769–782.
[8] K.S. Liu, L. Jiang, Metallic surfaces with special wettability, Nanoscale 3 (2011) 825–838.
[9] Y.Y. Yan, N. Gao, W. Barthlott, Mimicking natural superhydrophobic surfaces and grasping the wetting process: a review on recent progress in preparing superhydrophobic surfaces, Adv. Colloid Interface Sci. 169 (2011) 80–105.
[10] T.H. Her, R.J. Finlay, C. Wu, S. Deliwala, E. Mazur, Microstructuring of silicon with femtosecond laser pulses, Appl. Phys. Lett. 73 (1998) 1673–1675.
[11] M. Groenendijk, Fabrication of super hydrophobic surfaces by fs laser pulses, Laser Technol. 5 (2008) 44–47.
[12] F. Chen, D. Zhang, Q. Yang, J. Yong, G. Du, J. Si, F. Yun, X. Hou, Bioinspired wetting surface via laser microfabrication, ACS Appl. Mater. Interfaces 5 (2013) 6777–6792.
[13] A.Y. Vorobyev, C. Guo, Direct femtosecond laser surface nano/microstructuring and its applications, Laser Photon. Rev. 7 (2013) 385–407.
[14] F. Chen, D. Zhang, Q. Yang, X. Wang, B. Dai, X. Li, X. Hao, Y. Ding, J. Si, X. Hou, Anisotropic wetting on microstrips surface fabricated by femtosecond laser, Langmuir 27 (2010) 359–365.
[15] D.S. Zhang, F. Chen, Q. Yang, J.L. Yong, H. Bian, Y. Ou, J.H. Si, X.W. Meng, X. Hou, A simple way to achieve pattern-dependent tunable adhesion in superhydrophobic surfaces by a femtosecond laser, ACS Appl. Mater. Interfaces 4 (2012) 4905–4912.
[16] A.-M. Kietzig, S.G. Hatzikiriakos, P. Englezos, Patterned superhydrophobic metallic surfaces, Langmuir 25 (2009) 4821–4827.
[17] A.M. Kietzig, M.N. Mirvakili, S. Kamal, P. Englezos, S.G. Hatzikiriakos, Laser-patterned super-hydrophobic pure metallic substrates: Cassie to Wenzel wetting transitions, J. Adhes. Sci. Technol. 25 (2011) 2789–2809.
[18] B. Wu, M. Zhou, J. Li, X. Ye, G. Li, L. Cai, Superhydrophobic surfaces fabricated by microstructuring of stainless steel using a femtosecond laser, Appl. Surf. Sci. 256 (2009) 61–66.
[19] R. Jagdheesh, B. Pathiraj, E. Karatay, G. Romer, A.J.H. in't Veldt, Laser-induced nanoscale superhydrophobic structures on metal surfaces, Langmuir 27 (2011) 8464–8469.
[20] M. Tang, V. Shim, Z.Y. Pan, Y.S. Choo, M.H. Hong, Laser ablation of metal substrates for super-hydrophobic effect, J. Laser Micro Nanoeng. 6 (2011) 6–9.
[21] S. Moradi, S. Kamal, P. Englezos, S.G. Hatzikiriakos, Femtosecond laser irradiation of metallic surfaces: effects of laser parameters on superhydrophobicity, Nanotechnology 24 (2013) 415302.
[22] M.V. Rukosuyev, J. Lee, S.J. Cho, G. Lim, M.B.G. Jun, One-step fabrication of superhydrophobic hierarchical structures by femtosecond laser ablation, Appl. Surf. Sci. 313 (2014) 411–417.
[23] A.Y. Vorobyev, C. Guo, Multifunctional surfaces produced by femtosecond laser pulses, J. Appl. Phys. 117 (2015) 033103.
[24] F. Su, K. Yao, Facile fabrication of superhydrophobic surface with excellent mechanical abrasion and corrosion resistance on copper substrate by a novel method, ACS Appl. Mater. Interfaces 6 (2014) 8762–8770.
[25] A. Dunn, J.V. Carstensen, K.L. Wlodarczyk, E.B. Hansen, J. Gabzdyl, P.M. Harrison, J.D. Shephard, D.P. Hand, Nanosecond laser texturing for high friction applications, Opt. Lasers Eng. 62 (2014) 9–16.
[26] S. Moradi, P. Englezos, S.G. Hatzikiriakos, Contact angle hysteresis of non-flattened-top micro/nanostructures, Langmuir 30 (2014) 3274–3284.
[27] J. Drelich, E. Chibowski, D.D. Meng, K. Terpilowski, Hydrophilic and superhydrophilic surfaces and materials, Soft Matter. 7 (2011) 9804–9828.
[28] R.N. Wenzel, Resistance of solid surfaces to wetting by water, Ind. Eng. Chem. 28 (1936) 988–994.
[29] A.B.D. Cassie, S. Baxter, Wettability of porous surfaces, Trans. Faraday Soc. 40 (1944) 0546–0550.
[30] P. Bizi-bandoki, S. Valette, E. Audouard, S. Benayoun, Time dependency of the hydrophilicity and hydrophobicity of metallic alloys subjected to femtosecond laser irradiations, Appl. Surf. Sci. 273 (2013) 399–407.
[31] J. Long, M. Zhong, P. Fan, D. Gong, H. Zhang, Wettability conversion of ultrafast laser structured copper surface, J. Laser Appl. 27 (2015) S29107.
[32] G. McHale, N.J. Shirtcliffe, M.I. Newton, Super-hydrophobic and super-wetting surfaces: analytical potential? Analyst 129 (2004) 284–287.
[33] F.-M. Chang, S.-L. Cheng, S.-J. Hong, Y.-J. Sheng, H.-K. Tsao, Superhydrophilicity to superhydrophobicity transition of CuO nanowire films, Appl. Phys. Lett. 96 (2010) 114101.
[34] W. Barthlott, C. Neinhuis, Purity of the sacred lotus, or escape from contamination in biological surfaces, Planta 202 (1997) 1–8.
[35] T. Sun, G. Wang, L. Feng, B. Liu, Y. Ma, L. Jiang, D. Zhu, Reversible switching between superhydrophilicity and superhydrophobicity, Angew. Chem. Int. Ed. 43 (2004) 357–360.
[36] Y. Jiang, Z. Wang, X. Yu, F. Shi, H. Xu, X. Zhang, M. Smet, W. Dehaen, Self-assembled monolayers of dendron thiols for electrodeposition of gold nanostructures: toward fabrication of superhydrophobic/superhydrophilic surfaces and ph-responsive surfaces, Langmuir 21 (2005) 1986–1990.
[37] W. Choi, A. Tuteja, S. Chhatre, J.M. Mabry, R.E. Cohen, G.H. McKinley, Fabrics with tunable oleophobicity, Adv. Mater. 21 (2009) 2190–2195.